Lawrence Berkeley National Laboratory

Title
Stabilizing Liquids Using Interfacial Supramolecular Assemblies

Permalink
https://escholarship.org/uc/item/11r20981

Journal

ISSN

Authors
Gu, Peiyang
Luo, Xiaobo
Zhou, Shiyuan
et al.

Publication Date

DOI

Copyright Information

Peer reviewed

Relaxing Wrinkles in Jammed Interfacial Assemblies

Ganhua Xie,#*[a,b] Shipei Zhu,#[b] Paul Y. Kim,[b] Shubao Jiang,[a] Qinpiao Yi,[a] Pei Li,[c] Zonglin Chu,[a] Brett A. Helms[b,d] and Thomas P. Russell*[b,e,f]

[a]   State Key Laboratory for Chemo/Bio-Sensing and Chemometrics, College of Chemistry and Chemical Engineering, Hunan University, Changsha 410082, China
        E-mail: ganhuaxie@hnu.edu.cn
[b]   Materials Sciences Division, Lawrence Berkeley National Laboratory, One Cyclotron Road, Berkeley, CA 94720, USA
        E-mail: russell@mail.pse.umass.edu
[c]   Analytical Instrumentation Center, Hunan University, Changsha 410082, China
[d]   The Molecular Foundry, Lawrence Berkeley National Laboratory, One Cyclotron Road, Berkeley, CA 94720, USA
[e]   Polymer Science and Engineering Department, University of Massachusetts, Amherst, MA 01003, USA
[f]   Advanced Institute for Materials Research (AIMR), Tohoku University, 2-1-1 Katahira, Aoba, Sendai 980-8577, Japan
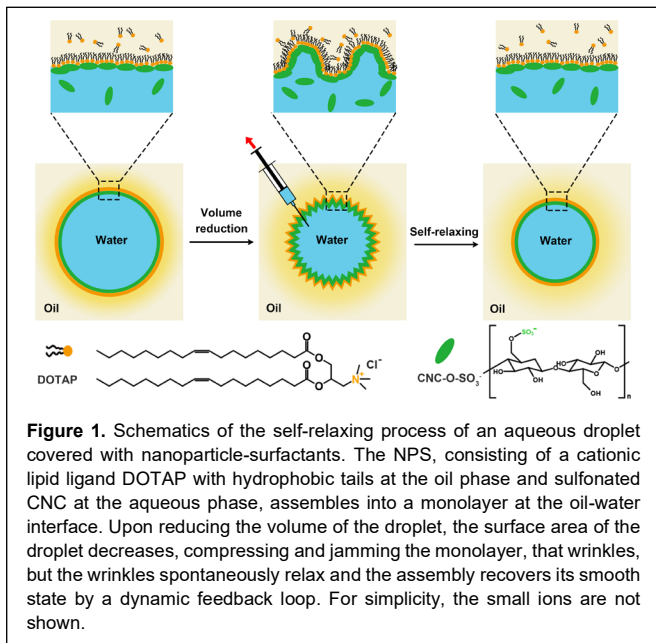#   These authors contributed equally to this work.

Abstract: Dynamic covalent bonding has emerged as a mean by which stresses in a network can be relaxed. Here, the strength of the bonding of ligands to nanoparticles at the interface between two immiscible liquids affect the same results in jammed assemblies of nanoparticle surfactants. Beyond a critical degree of overcrowding induced by the compression of jammed interfacial assemblies, the bonding of ligands to nanoparticles (NPs) can be broken, resulting in a desorption of the NPs from the interface. This reduces the areal density of nanoparticle surfactants at the interface, allowing the assemblies to relax, not to a fluid state but rather another jammed state. The relaxation of the wrinkles caused by the compression reflects the tendency of these assemblies to eliminate areas of high curvature, favoring a more planar geometry. This has enabled the generation of giant vesicular and multivesicular structures from these assemblies.

Introduction

Ageing of materials is, oftentimes, related to the relaxation of stresses, either globally or locally. Stresses exert a constant force on materials where the packing of atoms or molecules places the material in a non-equilibrium state and the system is striving to minimize energies associated with non-uniform densities, as found in heterogeneities in the density of a glassy materials, kinetically trapped during cooling.[1] In the case of polymer networks, stresses arise from the elastic retractive forces of chains stretched between entanglement points due to non-uniform distribution of crosslink points, for example.[2] The dynamic covalent or non-covalent bonding of network chains to junction points allows a system to be deformed, but the dynamic bonding enables the network to fully relax stresses by bond exchanges between the network chains and the junction points such that, when a network chain is released from a junction point, it relaxes, and then dynamically bonds to another junction point. As a result, the network, after relaxation, even though the bonding is re-arranged, is identical to the original undeformed network. Here, we introduce a similar concept to the interfacial packing of nanoparticle surfactants (NPSs), formed by the interfacial interactions between functionalized nanoparticles (NPs) in one fluid, and ligands dissolved in a second immiscible liquid, where multiple ligands anchor to the NP surface by electrostatic interactions. Here, rather than integrating dynamic covalent

bonding to form the NPS, we use the strength of the bonding of the ligands to the NP and the compressive force arising from the packing of the NPSs to affect a relaxation. The binding energy of NPSs to the interface is very much greater than that of NPs, consequently, assemblies of NPS, when compressed will jam, allowing non-equilibrium shapes of liquid domains decorated with NPSs to be indefinitely locked in a non-equilibrium state.[3] Breaking the jamming of the NPS requires the use of an external force, like shearing or an electric or magnetic field to physically force the NPSs to move and break the jam.[3d, 4] Alternatively, heating or adding a chemical to break the bonding of the ligands to the NPs can also be used where the ligands are solubilized in the one of the liquids and the NPs, with a very low binding energy to the interface, are dispersed in the second liquid.[5] This alleviates the crowding of the interface. The jamming of the assembly breaks, and the assemblies relax.

If, though, we could build-in a bonding of the ligands to the NPs that was sufficiently strong to enable the formation of NPSs to significantly reduce the interfacial tension and allow the assemblies to jam, but any additional applied stress would disrupt the NPS bonding, allowing in-plane stresses to relax and leave the assemblies in the initial relaxed jammed state, then we would have built-in an autonomous relaxation mechanism from one non-equilibrium state back to the original non-equilibrium, jammed state. While being akin to vitrimers in terms of relaxation and changes in the topology, where the compression of percolated pathways of NPSs that bear load play a role similar to that of the network chains stretched between crosslink points, here the NPS assemblies return to a jammed, non-equilibrium shape.[2c, 2d] Analogous to sandpiles that transit from one non-equilibrium jammed state to another as a consequence of a critical stress breaking a percolated pathway supporting the pile, with the NPS system, we can chemically define the stress where the surfactant-ligand bonding is disrupted, affording tunable control. These 2D jammed NPS assemblies, though asymmetric in nature,

Figure 1. Schematics of the self-relaxing process of an aqueous droplet covered with nanoparticle-surfactants. The NPS, consisting of a cationic lipid ligand DOTAP with hydrophobic tails at the oil phase and sulfonated CNC at the aqueous phase, assembles into a monolayer at the oil-water interface. Upon reducing the volume of the droplet, the surface area of the droplet decreases, compressing and jamming the monolayer, that wrinkles, but the wrinkles spontaneously relax and the assembly recovers its smooth state by a dynamic feedback loop. For simplicity, the small ions are not shown.

Figure 2. Interfacial property of the water-in-oil droplet stabilized by CNC-DOTAP NPSs. (a) Temporal evolution of interfacial tension of aqueous CNC dispersions (10 g/L, pH 7.94, aqueous droplet volume: ~40 μL) introduced to solutions of DOTAP with different concentrations ranging from 0 to 0.5 g/L in a mixed oil (silicone oil/hexadecane:1/1 (v/v)), illustrating control over the rate of NPS assembly at the interface. (b) Wrinkling behavior observed when decreasing the volume of a droplet cladded with interfacial NPSs (insert). As DOTAP concentration increases, the surface coverage increases and plateaus from 0.05 g/L. Scale bar, 1 mm.

behave similarly to lipid bilayers and represent an unusual type of liquid that has a bending rigidity. The NPS assemblies favor low curvature, opening an avenue to the generation of giant vesicular structures.
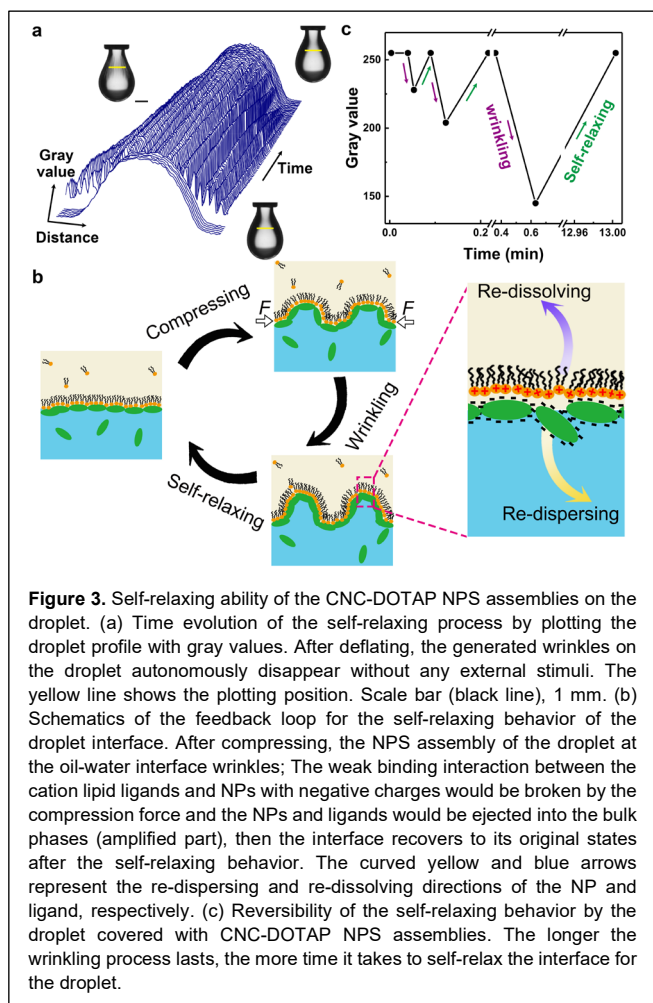
Results and Discussion

We describe a new platform to generate all-liquid constructs stabilized by the interfacial assembly of NPSs consisting of cationic lipids in an oil phase and NPs functionalized with negative charges in an aqueous phase. When the volume of the construct (here a droplet is used as a model) is reduced, a wrinkling of the assembly occurs that spontaneously relaxes by a dissipative process (**Figure 1**). A droplet of sulfonated cellulose nanocrystals (CNC), having diameters of 5~20 nm and lengths of 100~200 nm, in water was placed in a solution of 1,2-dioleoyloxy-3-(trimethylammonium)propane (DOTAP) chloride in a mixture of oils (silicone oil/hexadecane:1/1 (v/v)). With only sulfonated CNCs in the aqueous phase or only pure water, the interfacial tension (IFT) remains high at 26-27 mN/m, indicating that the interfacial activity of sulfonated CNC at the water-oil interface is quite low or non-existent. However, with CNCs in the aqueous phase and DOTAP in the oil phase, NPSs are produced by the electrostatic interactions between the tertiary amine of the DOTAP and sulfate functionality of the CNCs at the oil-water interface which has lower IFTs than that with only DOTAP at the oil phase (**Figure S1**). As shown in **Figure 2a**, at a CNC concentration of 10 g/L, for DOTAP concentrations < 0.005 g/L, only a modest decrease in the IFT is observed. For higher DOTAP concentrations, though, the reduction in the IFT is dramatic and, in fact, the IFT is so low that the droplet falls from the needle, since the energetic cost of distending the droplet is lower than the gravitational force pulling the droplet down. An estimate of the coverage of the droplet surface with NPSs can be obtained by decreasing the volume of the droplet (by withdrawal of the liquid in the droplet back into the needle) until the assembly first wrinkles. From the ratio of this volume to the original droplet volume, a rough estimate of the surface covered by the NPSs can be obtained. From **Figure 2b**, the surface coverage increases to
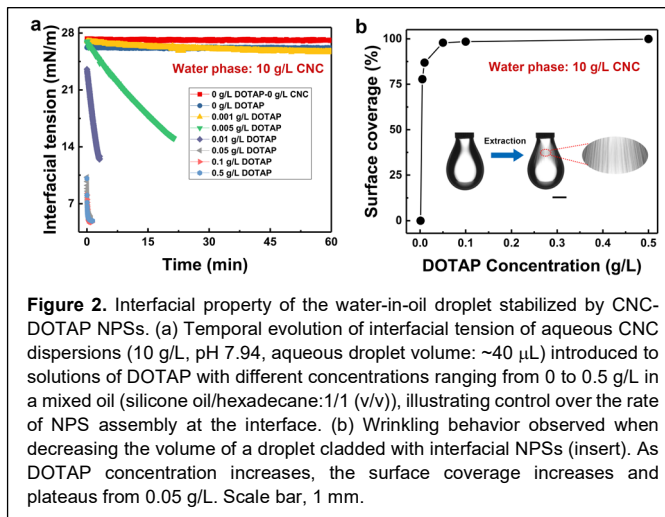
100% when the concentration of DOTAP is 0.005 g/L or higher. The surface of the droplet has a periodic wrinkling pattern, as observed in other systems.[3b, 3c, 4b, 6]

Usually, wrinkled assemblies of NPSs are jammed, and, absent external stimuli or additives, remain wrinkled indefinitely.[5b, 6d, 7] Here, though, the wrinkles first form and then rapidly relax (within ~5 s, see **Figure 3a**), due to a disruption of the bonding between the DOTAP and the NPs with both the DOTAP and NPs diffusing away from the interface (**Figure 3b**). Not only does this reduce the areal density of the particles at the interface but also locally breaks the jamming of the NPS in the regions of higher curvature. This allows the wrinkled assemblies to relax to a smooth, more planar interface. Withdrawing liquid from the new smooth droplet shows an immediate wrinkling, indicating that the surface coverage is again ~100%, and, as evidenced from measurements on magnetic NPs that will be discuss later, the NPS assemblies are jammed. Unless otherwise stated, the surface coverage of NPSs on the droplet is 100%. Consequently, the system relaxes from one jammed state to essentially the same jammed state during this relaxation, albeit with a reduction in the total volume. As shown in **Figure 3c**, repeated experiments on the wrinkling and recovery of the droplet interface shows that the bending modulus remains essentially unchanged, as evidenced by the invariance of the wrinkle wavelength (**Figure S2**).[3c] We note that when the droplet volume is slowly reduced, the amplitudes of the wrinkles are greater, and recovery slower, reflecting the dynamic interaction between DOTAP and CNC.

The importance of the bonding of the cationic lipid to the NP is manifest by replacing it with a zwitterionic lipid (1,2-dioleoyl-sn-glycero-3-phosphocholine (DOPC)). The bonding of the DOPC to the NPs is weaker than that of the DOTAP and, therefore, more easily disrupted. For aqueous droplets of CNC dispersions in contact with a solution of DOPC in the oil phase, wrinkling is not observed (**Figure S3**), even though the reduction in the interfacial tension was substantial, indicating a full coverage of the interface with DOPC. If DOTAP is added to the oil phase containing DOPC to generate mixed NPSs assemblies, the reduction and rate of reduction in the interfacial tension are commensurate with the DOPC fraction (**Figure S4**). However, while the pure DOTAP assemblies wrinkle, assemblies from mixtures with DOTAP fractions of 75% (25% DOPC) or less were never found to wrinkle, even when the droplet is completely extracted. Since the interaction of DOPC with the CNC is much weaker than DOTAP,

Figure 3. Self-relaxing ability of the CNC-DOTAP NPS assemblies on the droplet. (a) Time evolution of the self-relaxing process by plotting the droplet profile with gray values. After deflating, the generated wrinkles on the droplet autonomously disappear without any external stimuli. The yellow line shows the plotting position. Scale bar (black line), 1 mm. (b) Schematics of the feedback loop for the self-relaxing behavior of the droplet interface. After compressing, the NPS assembly of the droplet at the oil-water interface wrinkles; The weak binding interaction between the cation lipid ligands and NPs with negative charges would be broken by the compression force and the NPs and ligands would be ejected into the bulk phases (amplified part), then the interface recovers to its original states after the self-relaxing behavior. The curved yellow and blue arrows represent the re-dispersing and re-dissolving directions of the NP and ligand, respectively. (c) Reversibility of the self-relaxing behavior by the droplet covered with CNC-DOTAP NPS assemblies. The longer the wrinkling process lasts, the more time it takes to self-relax the interface for the droplet.

Figure 4. Modulating and functionalizing the covered assembly of the self-relaxing droplet by mixing nanoparticles. (a) Schematics of the functionalized assembly with tunability at the oil-water interface. The aqueous droplet with mixed sulfonated CNC and carboxylated MNP is dispersed into an oil solution with DOTAP. CNC and MNP particles competitively interact with DOTAP at the interface. By modulating the components of the nanoparticles in the aqueous phase, we can regulate the property of the monolayer assembly and endow it with some novel functions. For simplify, the small ions are not shown. (b) Images of performance transition of the skin from solid-like state to fluid-like state by increasing MNP concentration from 0 to 0.5 g/L (the concentrations of CNC and DOTAP are fixed at 10 g/L and 0.5 g/L, respectively). (c) Temporal evolution of interfacial tension of aqueous CNC and MNP mixture with different components (pH 7.94) introduced to solutions of DOTAP in the mixed oil (aqueous droplet volume: ~5.5 mL). As the MNP concentration increases, the interfacial tension of the droplet experiences a first increase and then decrease change, and the apparent surface coverage decrease from 100% to 0 (d).

ligand exchange is not expected, the suppression of the wrinkles may arise from a non-uniform distribution of DOPC and DOTAP. Carboxylated magnetic nanoparticles (MNPs, Fe_3O_4-COOH) form a solid-like NPS monolayer at the oil-water interface with amino-terminated polymer ligands dissolved in the oil phase and typical wrinkling behavior where the wrinkles do not relax is described.[4b, 8] However, if DOTAP is used instead of amino-terminated polymer ligands, over a pH range from 2.98 to 11.95 (**Figure S5**) with particle diameters ranging from 10 nm to 1000 nm (extracting rate: 20 µL/min) (**Figure S6**), no wrinkling is observed. It is interesting to note that when the rate of volume reduction was increased to 100 µL/min, a non-equilibrium structure was obtained (**Figure S7**), indicating a jamming of the NPSs formed by the DOTAP and MNPs and a kinetic trapping of the assemblies that locks in the shape of the droplet. Unlike unmodified CNCs that are surface active without the ligands,[9] carboxylated MNPs do not assemble at an oil-water interface in the absence of the ligands and are repelled from the interface. As previously reported, a droplet without an interfacial assembly of jammed MNPs is not expected to be ferromagnetic.[4b, 8] However, we find that a droplet covered with MNPSs formed from DOTAP and MNPs shows ferromagnetic properties (**Figure S8**), where the droplets will rotate in response to a rotating magnetic field, further confirming that the fluid-like MNPS layer is jammed at the interface. An equally interesting and more-visual example is the plasmonic liquid mirror generated by DOTAP and carboxylated gold NP (AuNP) assemblies at the oil-water interface.[10] Here, upon reduction of the droplet volume, rather than wrinkling, the droplet
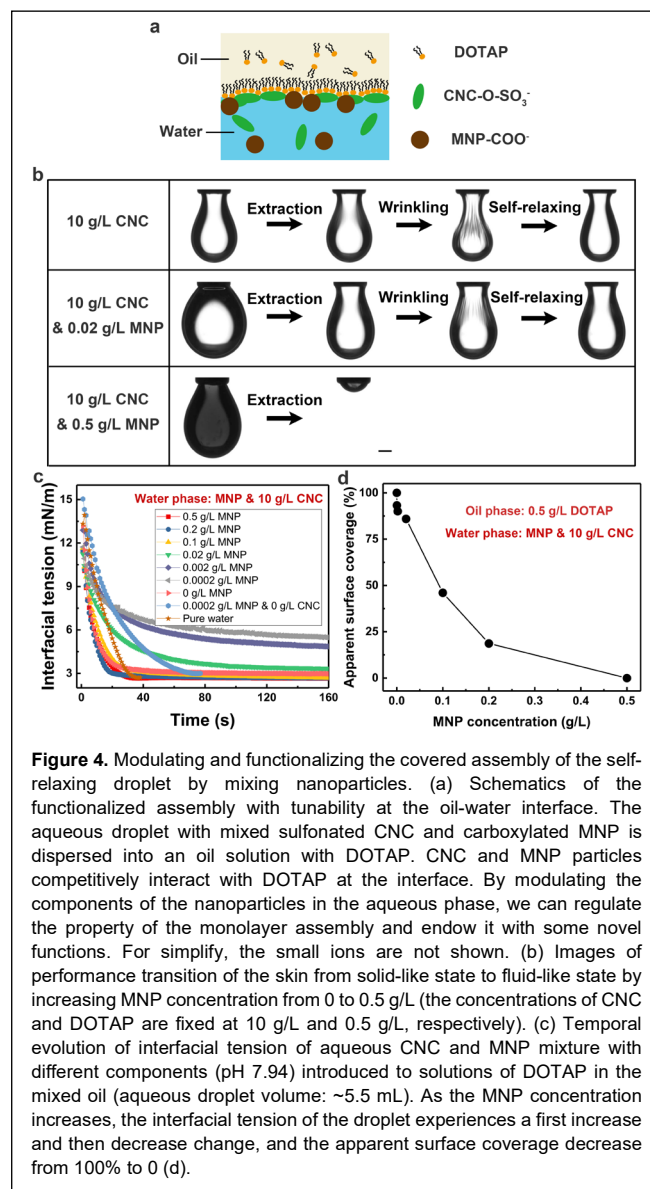
assumes an unusual, solid shape that could only happen if the assemblies were jammed. However, this shape returns to a classic droplet shape where the interfacial tension measured from the droplet shape is the same as that prior to the volume reduction (**Figure S6**). With carboxylated silica nanoparticles (SiNPs) interacting with DOTAP, though, wrinkling is observed, and, like the CNC system, the wrinkles relax (**Figure S6**). Consequently, for a broad range of NPs that interact with DOTAP at the water-oil interface, the assemblies formed can be jammed and these jammed assemblies can be deformed into a wrinkled or other solid-like shape, i.e. the assemblies clearly have a bending modulus,[3c] but the deformed assemblies fully relax, like a liquid, where the relaxation appears to arise from a disruption of the NPSs when they are compressed at the interface, most likely in areas of high curvature.

Due to the different interfacial behavior of CNCs and other NPs, an alternative strategy to manipulate the characteristics and functionality assemblies using DOTAP is to co-assemble NPs with different shape and/or inherent functionality. Assemblies from mixtures of CNC and MNP NPSs with DOTAP were prepared (**Figure 4a**). As indicated in **Figure 4b**, the assemblies show a gradual transition between a solid-like and fluid-like state
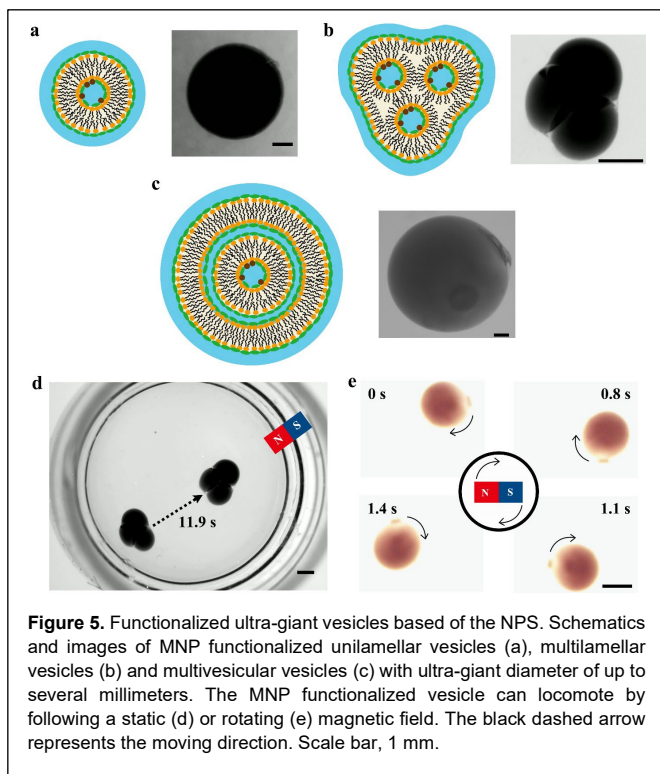
Figure 5. Functionalized ultra-giant vesicles based of the NPS. Schematics and images of MNP functionalized unilamellar vesicles (a), multilamellar vesicles (b) and multivesicular vesicles (c) with ultra-giant diameter of up to several millimeters. The MNP functionalized vesicle can locomote by following a static (d) or rotating (e) magnetic field. The black dashed arrow represents the moving direction. Scale bar, 1 mm.

as the MNP concentration increases from 0 to 0.5 g/L (with the DOTAP and CNC concentrations fixed at 0.5 g/L and 10 g/L, respectively). It is interesting to note that the interfacial tension increased from 2.97 mN/m for the pure CNC/DOTAP system to ~5.5 mN/m with the addition of 0.0002 g/L of MNPs which is, also well-above the interfacial tension of 2.69 mN/m with only 0.0002 g/L MNP/DOTAP system (**Figure 4c** and **Figure S9**). With increasing MNP concentration, the interfacial tension proportionately decreased to that for the pure MNP/DOTAP system as one would expect for uniform mixtures of the two components. The increase in the IFTs observed clearly indicates that the spherical, 30 nm diameter MNPs have disrupted the packing of the ellipsoid-shaped CNCs having diameters ranging from 5-20 nm, due to the size and shape disparity.[9a] The apparent surface coverage, actually the fractional reduction in the surface area when the assemblies begin to wrinkle, of the mixed systems decreases with increasing MNP concentration (**Figure 4d**). For the pure CNC system, wrinkling is observed immediately upon reducing the surface area indicating that the assemblies are easily jammed. However, upon introducing the MNPs to the CNC assemblies, the extent to which the assemblies must be contracted to induce jamming increases in an exponential manner with increasing MNP concentration and, at a concentration of ~0.2 g/L of MNPS mixed with 10 g/L CNC, the assemblies cannot be wrinkled, like that seen for the pure MNP-DOTAP system. It is apparent that the MNPs act like a plasticizer or diluent during the contraction of the assemblies increasing the free volume (actually "free area") of the CNC assemblies, increasing the amount of contraction required to jam the CNCs. Related to this is the variation in the wavelength pattern formed during contraction. With increasing MNP concentration, the wavelength of the assemblies decreases (**Figure S10**). For MNP concentration of 0.2 g/L, the wavelength of the assembly is so small that it is difficult to discern separate waves from the pictures due to its low resolution. For MNP concentration of 0.5 g/L, we did not observe any wrinkles during the extraction process.

From the results presented above, it is apparent that the assemblies of the CNCs with DOTAP are very much like the assemblies of lipid bilayers and polymersomes in their mechanical response. All represent systems that have the dynamics of liquids but exhibit a rigidity with a well-defined bending modulus. A significant difference of the CNC-DOTAP assemblies is that the assemblies are at an asymmetric water-oil interface, while the lipid bilayers and polymersomes are symmetric separating two aqueous or two oil-based liquids. Due to this similarity and the relaxation behavior of the CNC-DOTAP assemblies to eliminate regions of high curvature, i.e., the relaxation of the wrinkles to transit between two identical kinetically trapped assemblies, we investigated the use of bilayers of CNC-DOTAP assemblies to generate synthetic, vesicle-like assemblies (**Figure S11**). As shown in **Figure 5a**, a unilamellar vesicle was prepared, using components and structures akin to plant cells where the bilayers are stabilized by cellulose-dominated shells. Due to the stability of CNC-DOTAP NPSs, we were able to generate vesicular structures, at least 4.8 mm in size, which, to the best of our knowledge, is the largest synthetic lipid bilayer structure produced to date.[11] We note that by decreasing the droplet volume, the bilayer assembly can be wrinkled but, unlike the asymmetric single-layer assembly that can fully relax in 2 seconds (**Figure S12a**), the wrinkles only partially relax over a long period of 40 minutes (**Figure S12b**). By increasing the droplet volume, we measured the critical volume when the droplet breaks to be 1.86 V_0, where V_0 is the initial droplet volume (**Figure S13**). We were also able to generate extremely large multilamellar vesicles and multivesicular vesicles, as shown in **Figure 5b** and **Figure 5c**. The asymmetric bilayer structure allows us to further impart more function to the synthetic vesicles by, for example, the addition of MNPs. As shown in **Figure 5d** and **Figure 5e**, the functionalized vesicles show magnetotaxis and can be rotated in a rotating magnetic field. This result indicates that the assemblies are ferromagnetic in nature where a permanent magnetic moment can be imparted to the assemblies as we discussed previously for MNPs, provided the MNPs are jammed at the interface.[4b, 8] Such constructs have potential applications in drug delivery, cancer therapy and soft robots.[12] We demonstrated that such a functionalized vesicle platform is applicable to other NPs, which, we anticipate, will broaden potential applications in medical and materials applications.[12-13]

Conclusion

In summary, self-relaxation is one of the long-standing aims of bionics, applicable to both biological and synthetic material systems. To make constructs dynamic and multifunctional is a fundamental challenge for self-relaxing materials fabrication. The described method offers the possibility of designing a self-relaxing droplet system by using lipid-based NPSs. We have shown that different NPs, such as CNCs MNPs, AuNPs and SiNPs, can be used to fabricate dynamic assemblies on the droplets using single or multiple components, imparting different functions to the system. Cationic lipids make it possible to extend such synthetic system to soft robots, drug delivery and energy by evolving the water-in-oil droplets into extremely large, functionalized vesicles.
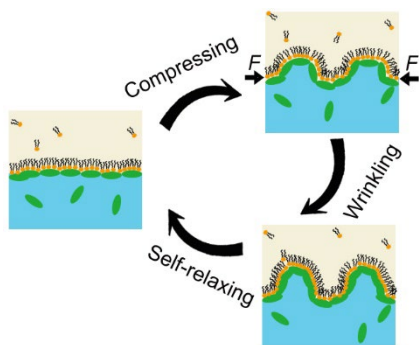
Acknowledgements

[1]   a) L. Cipelletti, L. Ramos, *J. Phys. Condens. Mat.* **2005**, *17*, R253; b) L. Berthier, G. Biroli, J.-P. Bouchaud, L. Cipelletti, W. van Saarloos, *Dynamical heterogeneities in glasses, colloids, and granular media, Vol. 150*, OUP Oxford, **2011**; c) L. Berthier, *J. Phys. Condens. Mat.* **2003**, *15*, S933.

[2]   a) W. Zou, J. Dong, Y. Luo, Q. Zhao, T. Xie, *Adv. Mater.* **2017**, *29*, 1606100; b) T. Maeda, H. Otsuka, A. Takahara, *Prog. Polym. Sci.* **2009**, *34*, 581-604; c) M. Capelot, M. M. Unterlass, F. Tournilhac, L. Leibler, *ACS Macro Lette.* **2012**, *1*, 789-792; d) D. Montarnal, M. Capelot, F. Tournilhac, L. Leibler, *Science* **2011**, *334*, 965-968.

[3]   a) J. Forth, P. Y. Kim, G. Xie, X. Liu, B. A. Helms, T. P. Russell, *Adv. Mater.* **2019**, *31*, e1806370; b) P.-Y. Gu, F. Zhou, G. Xie, P. Y. Kim, Y. Chai, Q. Hu, S. Shi, Q.-F. Xu, F. Liu, J.-M. Lu, T. P. Russell, *Angew. Chem. Int. Ed.* **2021**, *60*, 8694-8699; c) J. Forth, A. Mariano, Y. Chai, A. Toor, J. Hasnain, Y. Jiang, W. Feng, X. Liu, P. L. Geissler, N. Menon, B. A. Helms, P. D. Ashby, T. P. Russell, *Nano Lett.* **2021**, *21*, 7116-7122; d) M. Cui, T. Emrick, T. P. Russell, *Science* **2013**, *342*, 460-463.

[4]   a) A. Toor, J. Forth, S. Bochner de Araujo, M. C. Merola, Y. Jiang, X. Liu, Y. Chai, H. Hou, P. D. Ashby, G. G. Fuller, T. P. Russell, *Langmuir.* **2019**, *35*, 13340-13350; b) X. Liu, N. Kent, A. Ceballos, R. Streubel, Y. Jiang, Y. Chai, P. Y. Kim, J. Forth, F. Hellman, S. Shi, D. Wang, B. A. Helms, P. D. Ashby, P. Fischer, T. P. Russell, *Science* **2019**, *365*, 264-267.

[5]   a) Y. Jiang, R. Chakroun, P. Gu, A. H. Gröschel, T. P. Russell, *Angew. Chem. Int. Ed.* **2020**, *59*, 12751-12755; b) Z. Zhang, Y. Jiang, C. Huang, Y. Chai, E. Goldfine, F. Liu, W. Feng, J. Forth, T. E. Williams, P. D. Ashby, T. P. Russell, B. A. Helms, *Sci. Adv.* **2018**, *4*, eaap8045-8053.

[6]   a) Z. Li, Y. Shi, A. Zhu, Y. Zhao, H. Wang, B. P. Binks, J. Wang, *Angew. Chem. Int. Ed.* **2021**, *60*, 3928-3933; b) B. P. Binks, A. T. Tyowua, *Soft Matter* **2016**, *12*, 876-887; c) A. M. B. Rodriguez, B. P. Binks, *Soft Matter* **2020**, *16*, 10221-10243; d) C. Huang, Z. Sun, M. Cui, F. Liu, B. A. Helms, T. P. Russell, *Adv. Mater.* **2016**, *28*, 6612-6618; e) H. Sun, L. Li, T. P. Russell, S. Shi, *J. Am. Chem. Soc.* **2020**, *142*, 8591-8595 .

[7]   H. Sun, M. Li, L. Li, T. Liu, Y. Luo, T. P. Russell, S. Shi, *J. Am. Chem. Soc.* **2021**, *143*, 3719-3722.

[8]   X. Wu, R. Streubel, X. Liu, Y. Kim Paul, Y. Chai, Q. Hu, D. Wang, P. Fischer, P. Russell Thomas, *Proc. Natl. Acad. Sci. U. S. A.* **2021**, *118*, e2017355118.

[9]   a) X. Wu, Q. Yuan, S. Liu, S. Shi, T. P. Russell, D. Wang, *ACS Macro Lette.* **2019**, *8*, 512-518; b) K. Ito, M. Matsumoto, *Nanomaterials (Basel)* **2022**, *12*; c) C. Jiménez Saelices, M. Save, I. Capron, *Polym. Chem.* **2019**, *10*, 727-737.

[10]   a) A. A. Volkert, V. Subramaniam, M. R. Ivanov, A. M. Goodman, A. J. Haes, *ACS Nano* **2011**, *5*, 4570-4580; b) Y. Montelongo, D. Sikdar, Y. Ma, A. J. S. McIntosh, L. Velleman, A. R. Kucernak, J. B. Edel, A. A. Kornyshev, *Nat. Mater.* **2017**, *16*, 1127-1135.

[11]   a) T. Bhatia, P. Husen, J. Brewer, L. A. Bagatolli, P. L. Hansen, J. H. Ipsen, O. G. Mouritsen, *Biochim. Biophys. Acta Biomembr.* **2015**, *1848*, 3175-3180; b) A. C. Greene, D. Y. Sasaki, G. D. Bachand, *J. Vis. Exp.* **2016**, *111*, e54051-54057.

[12]   a) C. Hoskins, *J. Nanomed. Res.* **2014**, *1*, 4-16; b) V. P. Torchilin, *Nat. Rev. Drug Discov.* **2005**, *4*, 145-160.

[13]   a) D. Pornpattananangkul, S. Olson, S. Aryal, M. Sartor, C.-M. Huang, K. Vecchio, L. Zhang, *ACS Nano* **2010**, *4*, 1935-1942; b) J. Liu, A. Stace-Naughton, C. J. Brinker, *Chem. Commun.* **2009**, 5100-5102; c) M. Li, R. L. Harbron, J. V. Weaver, B. P. Binks, S. Mann, *Nat. Chem.* **2013**, *5*, 529-536; d) S. Mitragotri, D. G. Anderson, X. Chen, E. K. Chow, D. Ho, A. V.

Kabanov, J. M. Karp, K. Kataoka, C. A. Mirkin, S. H. Petrosko, J. Shi, M. M. Stevens, S. Sun, S. Teoh, S. S. Venkatraman, Y. Xia, S. Wang, Z. Gu, C. Xu, *ACS Nano* **2015**, *9*, 6644-6654; e) W. Wang, J. Luo, S. Wang, *Adv. Healthc. Mater.* **2018**, *7*, 1800484-1800511.

Entry for the Table of Contents

Autonomous stress-relaxing by dynamic jammed assemblies of nanoparticles and lipids at the interface was demonstrated. Such a lipid-based self-relaxing system may find applications in soft robots, medical and materials applications.

Institute and/or researcher Twitter usernames: ((optional))